Biomaterials 33 (2012) 7952–7958

Contents lists available at SciVerse ScienceDirect

Biomaterials

journal homepage: www.elsevier.com/locate/biomaterials

Surface localisation of photosensitisers on intraocular lens biomaterials for prevention of infectious endophthalmitis and retinal protection

Colin P. McCoy*, Rebecca A. Craig, Seana M. McGlinchey, Louise Carson, David S. Jones, Sean P. Gorman

School of Pharmacy, Queen's University Belfast, 97 Lisburn Road, Belfast BT9 7BL, UK

ARTICLE INFO

Article history:
Received 4 July 2012
Accepted 24 July 2012
Available online 11 August 2012

Keywords:
Bacterial adhesion
Copolymer
Endophthalmitis
Hydrogel
Intraocular lens
Photosensiter

ABSTRACT

Cataract surgery is one of the most commonly-practiced surgical procedures in Western medicine, and, while complications are rare, the most serious is infectious postoperative endophthalmitis. Bacteria may adhere to the implanted intraocular lens (IOL) and subsequent biofilm formation can lead to a chronic, difficult to treat infection. To date, no method to reduce the incidence of infectious endophthalmitis through bacterial elimination, while retaining optical transparency, has been reported. In this study we report a method to optimise the localisation of a cationic porphyrin at the surface of suitable acrylate copolymers, which is the first point of contact with potential pathogens. The porphyrin catalytically generates short-lived singlet oxygen, in the presence of visible light, which kills adherent bacteria indiscriminately. By restricting the photosensitiser to the surface of the biomaterial, reduction in optical transparency is minimised without affecting efficacy of singlet oxygen production. Hydrogel IOL biomaterials incorporating either methacrylic acid (MAA) or methyl methacrylate (MMA) co-monomers allow tuning of the hydrophobic and anionic properties to optimise the localisation of porphyrin. Physiochemical and antimicrobial properties of the materials have been characterised, giving candidate materials with self-generating, persistent anti-infective character against Gram-positive and Gram-negative organisms. Importantly, incorporation of porphyrin can also serve to protect the retina by filtering damaging shortwave visible light, due to the Soret absorption (λ_{max} 430 nm).

1. Introduction

Due to increasing life expectancies and changes in population structure, cataract surgery has become one of the most prevalent surgical procedures practiced in Western medicine [1]. Mature-onset cataracts develop when protein aggregation within the lens results in opacification and gradual loss of vision. Cataract surgery restores vision by removal of the natural crystalline lens and replacement with an implanted polymeric intraocular lens (IOL).

Following cataract extraction and IOL implantation, post-operative endophthalmitis (inflammation of the intraocular cavities) incidence in the UK is estimated conservatively to be between 0.1 and 0.2% [1–3]. Although occurring infrequently, endophthalmitis following cataract surgery is associated with significant postoperative morbidity. The main complication affecting at least 30% of patients is major visual loss, with blindness resulting in up to 18% of patients. Further negative implications for the patient include prolonged hospitalisation, and potential further surgery [4,5].

Bacterial adherence to an implanted IOL, and subsequent biofilm development, has been implicated in the pathogenesis of endophthalmitis. The Gram-positive coagulase-negative micrococcus *Staphylococcus epidermidis* is the most frequently cultured microorganism, however *Staphylococcus aureus* and anaerobic species have also been implicated [6]. The development of bacterial biofilm has negative implications on the outcome of treatment as bacteria in a biofilm are approximately 10–1000 times more resistant to antibiotics and biocides than their planktonic counterparts [7–9]. Currently, no IOLs are marketed which have strong, persistent anti-infective character.

Light-mediated antimicrobial strategies employing photosensitisers have been previously investigated for a number of pathogens including *Staphylococci* [10–12], viruses [13], and fungi [14]. Photoactivation of photosensitisers, typically porphyrins, results in the generation of a range of cytotoxic species, principally singlet oxygen ($^1O_2$), but also superoxide, hydroxyl and other radicals. The cytotoxicity of $^1O_2$ arises from indiscriminate oxidative reaction with any accessible macromolecule of the bacterial cell, so the development of bacterial resistance mechanisms is very

* Corresponding author. Tel.: +44 (0)28 9097 2081; fax: +44 (0)28 9024 7794.
E-mail address: c.mccoy@qub.ac.uk (C.P. McCoy).

0142-9612/$ – see front matter © 2012 Elsevier Ltd. All rights reserved.
http://dx.doi.org/10.1016/j.biomaterials.2012.07.052

difficult [15,16]. As the process of generation of the cytotoxic species is catalytic, the photosensitiser is not consumed in the process of cell killing, and can persist in providing a bacteriocidal effect for a prolonged period. While photosensitisers have proven antimicrobial efficacy, they have been used primarily in solution, and there is a compelling argument to develop methods to translate this activity to the surfaces of biomaterials.

Unlike previous work on PACT, uptake of the porphyrin by bacterial cells is not required. Rather, the $^1O_2$ generated by the porphyrin acts directly against bacteria adhering to the polymer surface, preventing subsequent bacterial adherence, the first stage of bacterial biofilm formation. As the lifetime of $^1O_2$ is in the range of 10^{-5}–10^{-6} s, the effective distance between the initial excitation event and cytotoxic damage is limited to a few micrometres, therefore preventing toxicity to normal tissue [5].

Recently, photoactivated porphyrin-impregnated hydrogels based on poly(2-(hydroxyethyl) methacrylate)-*co*-(methacrylic acid) copolymers have been reported [5,17]. To date, however, no studies have demonstrated localisation of photosensitiser on a polymer host whilst maintaining both antimicrobial activity and optical transparency to allow application in IOL biomaterials. In this paper, we describe methods to incorporate a tetracationic porphyrin, (tetrakis(4-*N*-methylpyridyl)porphyrin) (TMPyP), which binds electrostatically with methacrylate groups of the copolymer, in thin surface layers of a range of acrylate copolymers suitable for fabrication of IOLs using control of both hydrogel porosity and degree of electrostatic interaction between the biomaterial and the photosensitiser. This serves to give high surface concentrations of $^1O_2$ on excitation with visible light and allows the overall optical transparency to remain high for IOL applications. In addition to antimicrobial activity, an added benefit of TMPyP incorporation onto the surface of IOLs is the ability of this porphyrin to strongly absorb light in the blue/violet region of the visible spectrum (Soret band λ_{max} 430 nm). Much attention has been given to IOLs incorporating chromophores with the ability to absorb a certain amount of UV and/or blue light (<500 nm) in order to protect against photoreceptive retinal damage [18]. Exposure to such short wavelength light may be associated with an increased risk for age-related macular degeneration (AMD) and severe retinal damage [19,20]. Early IOLs allowed all UV and visible light to pass to the retina unrestricted, however UV-blocking lenses have been in use since the mid 1980s, and recently there has been support to increase the absorption spectrum of IOLs to reduce blue/violet light reaching the retina; such lenses show similar transmittance characteristics as a natural crystalline lens [18,21].

Here we have characterised the physicochemical and antimicrobial properties of TMPyP-incorporated acrylate hydrogel copolymers, and present candidate anti-infective, blue/violet-blocking, intraocular lens materials to improve patient outcomes in cataract surgery.

2. Materials and methods

2.1. Polymer preparation

Methyl methacrylate (MMA), methacrylic acid (MAA), 2-(hydroxyethyl)methacrylate (HEMA), benzoyl peroxide (BPO) and ethylene glycol dimethacrylate (EGDMA) were obtained from Aldrich.

Random copolymers composed of varying ratios of MMA:MAA:HEMA were prepared by free radical polymerisation, employing benzoyl peroxide (0.4% w/w) as an initiator and EGDMA (1% w/w) as a crosslinker as described previously [15]. Two series of copolymers were prepared; the first varies the MMA content at the expense of HEMA, while maintaining a constant MAA component, and the second varies the MAA content at the expense of HEMA, while maintaining a constant MMA component. The composition of copolymers prepared in this way is detailed in Tables 1 and 2. Included in Tables 1 and 2 are code definitions by which these copolymers are hereinafter identified.

Table 1
Polymers prepared by varying MMA content at the expense of HEMA, whilst MAA was maintained at 10%. Denoted hereafter as MMA series, with abbreviation codes as listed. EGDMA maintained constant at 1%. Percentages in table reflect the percentage composition of co-monomers in the remaining material.

MMA	MAA	HEMA	Abbreviation code
0	10	90	0MMA
5	10	85	5MMA
10	10	80	10MMA
15	10	75	15MMA

Impregnation of the hydrogels with TMPyP was performed by immersing samples into solutions of TMPyP (1 μg/ml) in phosphate buffered saline at pH 7.4 for 2 min, followed by washing with, and soaking in deionised water for seven days.

2.2. Thermal analysis of untreated polymers

Glass transition temperatures of untreated polymers were determined using a TA instruments 100 Modulated Differential Scanning Calorimeter (TA Instruments Ltd, Crawley, West Sussex, UK) with an attached refrigerated cooling system unit. A modulation amplitude of ±0.70 °C every 50 s was applied, with a 2 °C min^{-1} underlying heating rate. Heat flow was calibrated using an indium standard, and the heat capacity by means of a sapphire standard. Nitrogen was used as the purge gas, with a flow rate of 50 mL min^{-1} through the DSC cell. Standard aluminum pans were used, with the mass of each empty sample pan matching the mass of the empty reference pan to ±0.1 mg.

2.3. Determination of equilibrium water content

Coplymer samples were dried to a constant weight and then placed in distilled water at room temperature. Swelling of the samples was monitored by weighing at regular time intervals, after removing any surface water by blotting on tissue paper, until samples reached a constant hydrated weight. The equilibrium water content was calculated using Eq. (1):

$$EWC = [(W_2 - W_1)/W_2] \times 100 \quad (1)$$

where EWC is the equilibrium water content (%), W_2 is the mass of the sample after water absorption, and W_1 is the mass of dried gel.

2.4. Confocal laser scanning microscopy

Distribution of TMPyP in the hydrogels was characterised by visualising a cross-section of the relevant material using a Lecia TCS SP2 Confocal Laser Scanning Microscope (Lecia Microsystems, Wetzlar, Germany). The wavelength of excitation was 514 nm, generated by an Argon/Argon Krypton laser, and emission was monitored between 600 and 720 nm. 514 nm was selected as the wavelength of excitation due to its proximity to a Q band of TMPyP. The pinhole size and photomultiplier voltage were kept constant throughout the experiments.

2.5. UV–visible spectroscopic analysis

UV–visible absorbance measurements were obtained using a Perkin Elmer Lambda 650 UV–visible spectrometer coupled with UVWinLab software (Perkin Elmer, USA), enabling characterisation of total uptake of TMPyP. Spectra were recorded between 390 and 700 nm to permit visualisation of the Soret and Q bands of TMPyP. TMPyP loading was determined through measurement of absorbance at the peak maximum of the Soret band (430 nm). This was translated into quantitative TMPyP content per unit area by rearrangement of the Beer Lambert law. Assessment was made in quintuplicate for each material.

Table 2
Polymers prepared by varying MAA content at the expense of HEMA, whilst MMA was maintained at 5%. Denoted hereafter as MAA series, with abbreviation codes as listed. EGDMA maintained constant at 1%. Percentages in table reflect the percentage composition of co-monomers in the remaining material.

MAA	MMA	HEMA	Abbreviation code
0	5	95	0MAA
10	5	85	10MAA
20	5	75	20MAA
30	5	65	30MAA

2.6. Tensile analysis

The mechanical properties of untreated and TMPyP-impregnated polymers in the swollen state were determined using a Stable MicroSystems TA-XT Plus Texture Analyzer (Goldaming, Surrey, UK) as previously described [23–27]. Dumbbell shaped samples were cut from the hydrogels and fixed between the mobile upper and static lower clamps of the texture analyzer. The upper clamp was raised at a cross-head speed of 1.0 mm s^{-1} until sample fracture occurred, and at least five replicates of each analysis were performed. The mechanical properties of the samples (ultimate tensile strength (UTS), Young's modulus, and strain at failure) were calculated from the resultant stress–strain relationship.

2.7. Microbiological assessment

Materials were challenged with two relevant organisms – the Gram-positive *S. aureus* NCTC 10788 and Gram-negative *Pseudomonas aeruginosa* NCTC 12924, and the percentage adherence relative to untreated control materials (where TMPyP is not incorporated) were calculated. Copolymer samples were cut into discs (5 mm diameter) and placed on an absorbent sterile pad soaked in phosphate buffered saline (PBS), placed within a sterile petri dish, to avoid dehydration during light exposure. 10 μl of bacterial suspension in PBS (10^8 cfu/ml) was placed onto the discs such that each received an inoculum of approximately 10^3 cfu per disc. In the case of *P. aeruginosa*, no recovery of adhered bacteria was achieved following a 10^3 cfu inoculum on each disc, therefore to allow assessment of the porphyrin activity, this was increased to either 10^4 cfu or 10^5 cfu, as necessary until adherence could be quantified.

The discs were incubated at 37 °C for 10 min to allow the bacteria to adhere, transferred to a dry absorbent pad and any non-adhered bacteria were removed by washing with 1 mL sterile PBS. The discs were then transferred to a fresh PBS saturated pad within a sterile petri dish, and exposed for 1 h to light from a 250 W halogen bulb, or kept in the dark (dark controls) at a distance of 24 cm. Bacterial adherence to one side of the sample disc only was examined. The intensity of the light used was 8.91 mW cm^{-2}. Following light exposure, discs were placed in bijoux bottles containing 1.5 mL quarter strength Ringer's solution (QSRS), sonicated for 10 min, and vortexed for 30 s to remove adherent organisms. Numbers of previously adhered viable organisms surviving on the discs were determined by serial dilution of the QSRS, followed by plating out onto Mueller–Hinton Agar (MHA) as reported previously [17].

2.8. Statistical analysis

All experiments were performed in at least quintuplicate and results expressed as mean ± standard deviation. Statistical differences were evaluated using ANOVA, with the exception of the microbiological studies where the non-parametric Kruskal–Wallis test for multiple samples was utilised. In all cases a probability of $p \leq 0.05$ denoted significance.

3. Results

3.1. Thermal analysis

Glass transition temperatures (T_g) of untreated copolymers are shown in Table 3. All copolymers exhibited a single, smooth glass transition, illustrating that true copolymers were formed. An increasing T_g was observed in the MAA series, corresponding to an increasing MAA component in the copolymer, from 103.88 °C (0MAA), through to 150.46 °C (30MAA). No significant alteration in T_g was observed in the MMA series with increasing MMA component.

Table 3
Glass transition temperatures of untreated copolymers.

Polymer	Glass transition temperature T_g (°C)
0MMA	123.95
5MMA	120.96
10MMA	123.49
15MMA	121.81
0MAA	103.88
10MAA	120.96
20MAA	140.10
30MAA	150.46

3.2. Equilibrium water content

The equilibrium water content (EWC) was determined for both the MMA and MAA copolymer series. It is anticipated that an increase in the MMA component would impart a corresponding increase in the hydrophobic nature of the material, due to polyelectrolyte repulsion and subsequent expansion of the hydrogel network. This is reflected in the EWC values obtained for both control samples (without TMPyP incorporation), and TMPyP treated samples (Table 4). In both instances, the EWC was reduced with a corresponding increase in the hydrophobic MMA component of the copolymer. The data in Table 4 also illustrate a general trend for increasing EWC with increasing MAA component, which is consistent with the hydrophilic nature of MAA. In general, incorporation of TMPyP has no significant effect on the EWC of the copolymers. However, modest increases in EWC are observed for copolymers containing higher amounts of MAA upon TMPyP incorporation.

3.3. Confocal laser scanning microscopy

A representative confocal micrograph and depth profile is shown in Fig. 1a and b), respectively. TMPyP depth penetration data for all copolymers is given in Table 5. Depth of penetration varied between 18 μm and 40 μm, with the least TMPyP penetration depth exhibited by 10MMA. Increasing MAA content, which would provide additional points for electrostatic interaction between the anionic MAA and the cationic photosensitiser, did not further reduce the penetration of TMPyP, however increasing MMA content reduced the penetration of TMPyP. This observation is likely due to the increasing hydrophobic component of the copolymer impeding the penetration of TMPyP.

3.4. UV–visible spectroscopic analysis

Analysis of copolymers by UV spectroscopy provided a measure of the total loading of TMPyP per unit area of polymer. TMPyP loading was determined through measurement of absorbance at the peak maximum of the Soret band (430 nm). A positive correlation was observed between increasing MMA content and increased TMPyP uptake by the polymer, however no clear trend was observed in the MAA series. Overall, the MMA series showed a greater uptake of TMPyP than the MAA series, displaying

Table 4
Equilibrium water content (EWC) of both MMA and MAA copolymer series. Water content is expressed as a percentage of the total hydrated polymer weight.

Copolymer		Equilibrium water content (%)
Controls	0MMA	59.95 ± 1.16
	5MMA	47.82 ± 4.10
	10MMA	48.19 ± 2.81
	15MMA	40.64 ± 0.88
TMPyP treated	0MMA	57.11 ± 1.57
	5MMA	54.74 ± 2.52
	10MMA	47.09 ± 2.52
	15MMA	42.15 ± 1.25
Controls	0MAA	45.71 ± 0.80
	10MAA	40.24 ± 1.43
	20MAA	41.21 ± 4.80
	30MAA	44.02 ± 3.71
TMPyP treated	0MAA	47.94 ± 3.73
	10MAA	116.62 ± 17.01
	20MAA	56.02 ± 0.74
	30MAA	59.92 ± 5.03

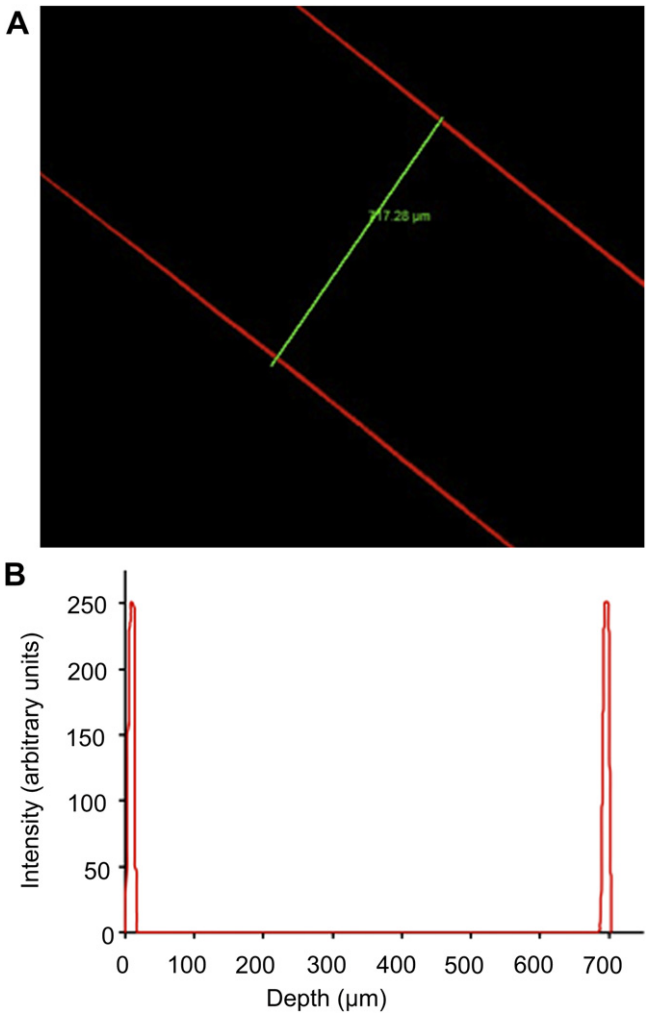

Fig. 1. A) Confocal scanning microscopy image of a TMPyP-impregnated 10MAA polymer. Line is drawn perpendicular to edges of polymer and corresponds with representative profile. B) Cross-sectional profile of the fluorescence of a TMPyP-incorporated 10MAA film measured by confocal laser fluorescence microscopy.

a maximum uptake of 5.78 ± 0.10 μg cm^{-2} compared to the maximum in the MAA series of 4.22 ± 0.03 μg cm^{-2}.

Optical transmittance of the TMPyP loaded samples was determined by analysis of the average percentage transmittance of the material over the visible region of the electromagnetic spectrum (390–700 nm) (Table 6). The average transmittance across the visible spectrum is reduced with increased TMPyP uptake, as is to be expected, with the lowest value for average transmittance of 72.87 ± 0.96% observed for 15MMA, which is the copolymer with

Table 5
Depth of penetration of TMPyP in treated copolymers, determined using confocal fluorescence microscopy.

Polymer	Depth of TMPyP penetration (μm) ± sd
0MMA	29.76 ± 1.28
5MMA	26.26 ± 8.96
10MMA	18.24 ± 2.18
15MMA	33.26 ± 16.4
0MAA	29.79 ± 0.00
10MAA	24.58 ± 3.37
20MAA	44.79 ± 10.00
30MAA	30.18 ± 17.57

Table 6
Total loading of TMPyP per cm^2 for each copolymer and percentage light transmission, averaged across the visible range (390–700 nm).

Polymer	Mass of TMPyP (μg/cm^2) ± sd	% Transmission ± sd
0MMA	3.78 ± 0.06	92.49 ± 4.01
5MMA	4.22 ± 0.03	85.74 ± 0.22
10MMA	5.34 ± 0.09	87.84 ± 0.35
15MMA	5.78 ± 0.10	72.87 ± 0.96
0MAA	2.87 ± 0.10	91.18 ± 2.25
10MAA	4.22 ± 0.03	85.74 ± 0.22
20MAA	2.49 ± 0.11	84.64 ± 1.23
30MAA	3.97 ± 0.05	77.78 ± 1.50

the highest loading of TMPyP. It must be mentioned that these values of percentage transmittance in the range of 390–700 nm are largely influenced by the strong absorption of the TMPyP Soret band at 430 nm, with the remainder of the spectrum remaining at, or close to, a low baseline transmission (>90%). In addition to the antimicrobial benefits of TMPyP incorporation onto the surface of IOLs, this reduction in optical transmission, specifically at the violet region (400–440 nm) may also have an important, advantageous function to protect the eye from wavelengths of light that contribute little to vision, yet are potentially harmful to the retina. Several IOLs in current commercial production and clinical use include chromophores, reducing the transmittance of ultraviolet and blue light, and show similar transmission spectra of the natural crystalline adult lens [18,21].

3.5. Tensile analysis

The mechanical properties of both series of copolymers, TMPyP-impregnated and untreated, are illustrated in Fig. 2. In untreated copolymers, increasing the MMA component resulted in a corresponding increase in ultimate tensile strength (UTS), and incorporation of TMPyP into the MMA series did not significantly affect UTS values in comparison to the untreated material. The MAA series also shows an increase in UTS with increasing MAA component, however, incorporation of TMPyP causes a modest reduction in UTS in comparison to the untreated material, which is most pronounced in the 30MAA copolymer. The inclusion of MAA in a copolymer is commonly used to increase water content due to its high hydrophilicity. This increase in water content would normally serve to decrease the UTS due to increased porosity of the material. In these copolymers, however, it is likely that MAA binds to MMA contained within the copolymer, wherein the ionic carboxylate moiety of MAA interacts with the partial positive charge of the MMA carboxyl carbon, with this effect being more pronounced in copolymers with higher MAA content. There is a trend in both the untreated MMA and MAA series for an increasing Young's modulus with an increasing MMA and MAA component, respectively. Incorporation of TMPyP serves to reduce the Young's modulus in comparison to the corresponding untreated copolymer, most dramatically in the case of 30MAA (52.09 ± 4.74 MPa for untreated material reduced to 0.91 ± 0.13 when TMPyP-incorporated). This suggests the incorporation of TMPyP in the 30MAA copolymer produces a flexible material that may assist in the development of a foldable IOL, requiring a much smaller surgical incision for insertion than that required for a rigid inflexible lens.

3.6. Bacterial adherence studies

Fig. 3 shows the bacterial adherence of *S. aureus* and *P. aeruginosa* to copolymers studied. With the exception of the 30MAA copolymer, bacterial adherence to all samples was significantly reduced under light conditions, in comparison to the

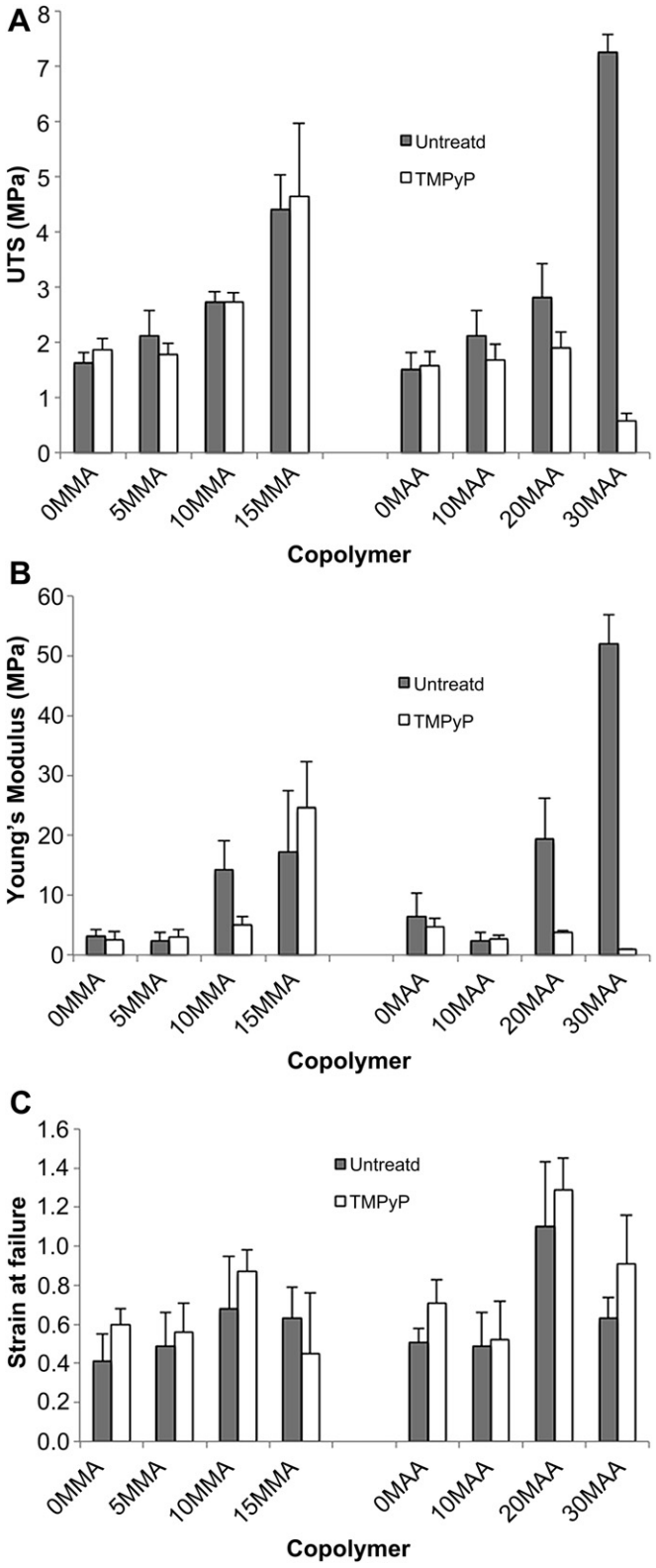

Fig. 2. A) Ultimate tensile strength (UTS), B) Young's modulus, and C) strain at failure for untreated and TMPyP-impregnated copolymers. Error bars represent standard deviations.

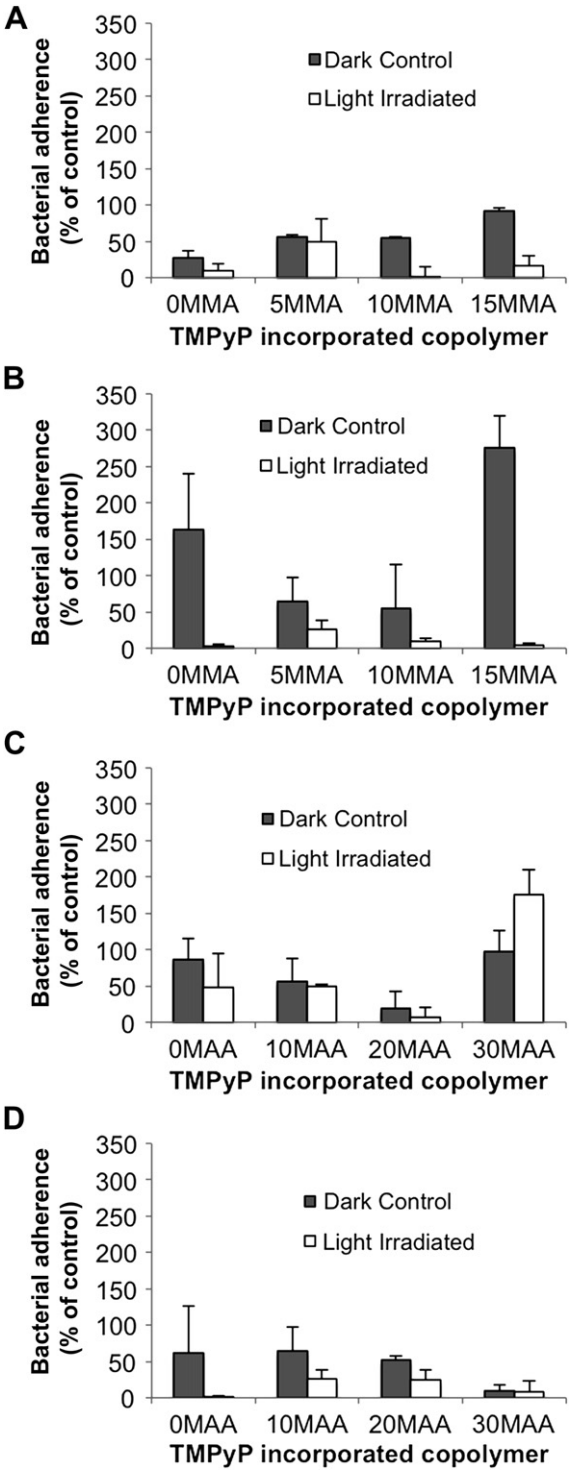

Fig. 3. Bacterial adherence of *S. aureus* and *P. aeruginosa* to TMPyP-incorporated copolymers under dark and light irradiated conditions. A) Adherence of *S. aureus* to MMA series. B) Adherence of *P. aeruginosa* to MMA series. C) Adherence of *S. aureus* to MAA series. D) Adherence of *P. aeruginosa* to MAA series. Error bars represent standard deviations.

corresponding dark control. Between copolymer compositions, however, there is no clear correlation between the degree of observed photodynamic antimicrobial activity of TMPyP-incorporated material surfaces.

It is not fully understood, and therefore difficult to predict, how the physicochemical properties of a biomaterial will influence bacterial adhesion, which may be a function of both material physical properties, and the bacterial characteristics, with different bacterial strains and species displaying varying abilities to adhere

to particular substrata [28,29]. It is clear from the data in Fig. 3, that under dark conditions adherence to the several of the TMPyP-incorporated copolymers is increased dramatically above that of the corresponding material control. Specifically, *P. aeruginosa* adherence to 0MMA and 15MMA under dark conditions (Fig. 3B), increased bacterial adherence to 162.73 ± 78.03% and 275.74 ± 44.39%, respectively. Interestingly, while these materials appeared to promote adherence under dark conditions, they also produced the most pronounced photodynamic antimicrobial properties under light irradiation. Compared to control material not incorporating TMPyP, adherence of *P. aeruginosa* was 2.90 ± 2.99% for light irradiated TMPyP-incorporated 0MMA, and 3.79 ± 3.43% for light irradiated TMPyP-incorporated 15MMA. The apparent ability of rod-shaped *P. aeruginosa* to form a close interaction with these TMPyP-incorporated materials may explain the successful reduction of adherence under light irradiation, given the fact that photodynamic microbial damage relies on close proximity and high level of interaction of the photosensitiser and the biomolecular target [22].

Strong light-induced antimicrobial activity was also observed against *S. aureus* on TMPyP-incorporated 10MMA (1.72 ± 1.82% of control), and against *P. aeruginosa* on TMPyP-incorporated 0MMA (1.03 ± 1.79% of control).

4. Discussion

p(HEMA-*co*-MAA-*co*-MMA) materials were selected for study due to the presence of negatively-charged pendant groups to facilitate electrostatic attachment of the tetracationic porphyrin, TMPyP. Incorporation of TMPyP on the lens surface is intended to impart antimicrobial properties to the material through the photodynamic generation of bactericidal reactive oxygen species, and also serves to protect the retina from damaging short wavelength visible light, due to its strong Soret absorption band (λ_{max} 430 nm). Modification of either the MMA or MAA content resulted in alteration either of polymer hydrophobicity or the relative number of available electrostatic binding sites, respectively, with the aim of modifying the ingress of TMPyP into the polymer. The prepared materials were fully characterised to provide a description of their physical, chemical, and microbiological properties.

The true copolymer nature of the prepared materials was displayed by the presence of a single T_g for each material. The increase in T_g with increasing MAA content is attributable to the higher T_g of MAA (190 °C) in comparison to MMA and HEMA (100 and 110 °C, respectively). Due to the proximity of the T_g of MMA to that of HEMA, negligible variation in the copolymer T_g of the MMA series was observed with alterations of MMA content. The T_g values of these copolymer blends indicate a rigid, inflexible material at body temperature. While there are advantages to developing intraocular lenses with low T_g temperatures (<37 °C), such as for foldable IOLs that may be surgically inserted through a smaller incision, the values obtained in this study are comparable to poly(methyl methacrylate) (PMMA), the most widely used IOL material, that possesses a T_g in the region of 113–119 °C.

UV–visible spectroscopic analysis demonstrates a larger uptake of TMPyP in the MMA series, however this was not to the detriment of the degree of surface localisation. Rather, decreased penetration into the bulk polymer, and therefore improved surface localisation, was observed. The correlation between increasing MMA content and decreasing depth of penetration in the MMA series highlights the efficacy of MMA to form a copolymer with an increased hydrophobic character (as demonstrated by equilibrium water content), hence causing a decrease in the porosity of the copolymer, and thus ingress of porphyrin during incorporation. An absence of a clear trend between MAA concentration and total TMPyP loading suggests that two opposing factors operate for these materials; while increasing the number of available electrostatic binding sites increases surface localisation, hydrogel expansion due to polyelectrolyte repulsion between proximate carboxylate groups serves to increase the porosity of the hydrogel, and permit more rapid penetration of sensitiser into the hydrogel bulk.

Optical transparency in the region of porphyrin absorbance is reduced in all materials, however as this is a small range of the visible spectrum, the overall impact on visual acuity should not be significant. Advantageously, TMPyP has a wavelength of maximum absorbance in the copolymers at 430 nm (the Soret band), which gives the candidate IOL materials blue/violet-blocking properties, protecting the eye against potential photodamage [18].

The increase in tensile strength through the MMA series is attributed to the smaller size of MMA in comparison to the other co-monomers, leading to tighter inter-chain packing, and enhanced hydrophobic bonding within the hydrogel. Consequently, more energy was required for bond breakage and fracture of the material. The decreased mechanical strength of TMPyP-incorporated MAA copolymers, particularly at high MAA concentrations may be explained by the greater depth of penetration of TMPyP into these materials, as exemplified by the confocal data. This facilitated a greater effect on the bulk polymer, leading to increased disruption of the polymer chains and thus a change in mechanical properties. In terms of IOL design, this is not necessarily a negative observation, as an IOL showing good flexibility can be placed using a less invasive surgical technique. TMPyP incorporation did not significantly alter the mechanical properties of the MMA series, which is as expected due to the minimal degree of penetration into the bulk, and therefore lack of effect on polymer chain arrangement.

Microbiological analysis demonstrated the efficacy of TMPyP-impregnated materials when compared to untreated control materials, with a greater reduction in bacterial adherence observed in light conditions for each material, confirming the antimicrobial action of reactive oxygen species generated by the incorporated porphyrin on photoactivation. The observed dark activity of the materials is probably related either to the alteration of the surface of the materials on porphyrin impregnation as previously reported [5], or to interaction with and disruption of the bacterial cell membrane due to the high charge of TMPyP molecules [30–34]. The non-adherence of *P. aeruginosa* at 10^3 cfu per disc to any of the impregnated or untreated materials indicates an inherent resistance to adherence of this bacterial strain. This may, in part, be conferred by the opposing negative charges of the material surface and the bacterial cell wall, which has a comparatively greater negative charge density than *S. aureus*. Clearly, this is a favourable property as Gram-negative infections are known to be significantly more difficult to treat, and are associated with poor visual outcome [35]. While increasing the loading to 10^4 or 10^5 cfu per disc provided a pathogen challenge above that likely to be encountered clinically, assessment of the antimicrobial activity of materials was possible. Despite this increased bacterial challenge, the efficacy of the porphyrin is evident, with strong reductions in adherence in light conditions. While adherence of *P. aeruginosa* to TMPyP-incorporated 0MMA and 15MMA was promoted under dark conditions, the apparent strong association of the bacterial cell with the material served to promote the photodynamic bactericidal effect, likely due to the close interaction of photosensitiser and the bacterial target. The consistency of performance by 10MMA in light conditions against both *S. aureus* and *P. aeruginosa* suggests it to have properties useful for reducing or preventing bacterial adherence in physiological conditions, and therefore for minimising the risk of biofilm formation and potentially the occurrence of IOL-related postoperative endophthalmitis.

5. Conclusions

A simple method of obtaining a high, localised concentration of photosensitiser at the surface of polymeric materials has been demonstrated, whilst maintaining optical transparency. The results suggest that the MMA series of materials possess more favourable properties, notably high porphyrin loading and high localisation at the surface of the materials, in addition to highly significant reductions in bacterial adherence on exposure to light. Of the materials examined, the most promising was 10MMA, displaying superior surface localisation of TMPyP and appropriate mechanical properties, in addition to excellent anti-infective properties. When applied to ophthalmological devices such as IOLs, the potential benefits of these materials to the patient are numerous, with the removal of the necessity for further pharmacological or invasive surgical treatment, which may otherwise be required following development of postoperative endophthalmitis. The ability of TMPyP to absorb short wavelength light in the blue/violet region of the visible spectrum offers the additional benefit of protection against photoreceptive retinal damage.

Acknowledgements

We acknowledge funding for this work from the Department for Employment and Learning (Northern Ireland). The authors thank Stef McGrath for technical assistance.

References

[1] ESCRS Endophthalimitis Study Group. Prophylaxis of postoperative endophthalmitis following cataract surgery: results of the ESCRS multicenter study and identification of risk factors. J Cataract Refract Surg 2007;33:978–88.
[2] Taban M, Behrens A, Newcomb R, Nobe M, Saedi G, Sweet P. Acute endophthalmitis following cataract surgery – a systematic review of the literature. Arch Ophthalmol 2005;123(5):613–20.
[3] West E, Behrens A, McDonnell P, Tielsch J, Schein O. The incidence of endophthalmitis after cataract surgery among the US medicare population increased between 1994 and 2001. Ophthalmology 2005;112(8):1388–94.
[4] Parsons C, Jones D, Gorman S. The intraocular lens: challenges in the prevention and therapy of infectious endophthalmitis and posterior capsular opacification. Expert Rev Med Devices 2005;2(2):161–73.
[5] Brady C, Bell SEJ, Parsons C, Gorman SP, Jones DS, McCoy CP. Novel porphyrin-incorporated hydrogels for photoactive intraocular lens biomaterials. J Phys Chem B 2007 01/01;111(3):527–34.
[6] Kresloff MS, Castellarin AA, Zarbin MA. Endophthalmitis Surv Ophthalmol 1998;43(3):193–224.
[7] Mah TF, O'Toole GA. Mechanisms of biofilm resistance to antimicrobial agents. Trends Microbiol 2001;9(1):34–9.
[8] Elder M, Stapleton F, Evans E, Dart J. Biofilm-related infections in opthalmology. Eye 1995;9:102–9.
[9] Smith A. Biofilms and antibiotic therapy: is there a role for combating bacterial resistance by the use of novel drug delivery systems? Adv Drug Deliv Rev 2005;57(10):1539–50.
[10] Orenstein A, Klein D, Kopolovic J, Winkler E, Malik Z, Keller N. The use of porphyrins for eradication of *Staphylococcus aureus* in burn wound infections. FEMS Immunol Med Microbiol 1997;19(4):307–14.
[11] Griffiths M, Wren B, Wilson M. Killing of methicillin-resistant *Staphylococcus aureus* in vitro using aluminium disulphonated phthalocyanine, a light-activated antimicrobial agent. J Antimicrob Chemother 1997;40(6):873–6.
[12] Sharma M, Visai L, Bragheri F, Cristiani I, Gupta P, Speziale P. Toluidine blue-mediated photodynamic effects on staphylococcal biofilms. Antimicrob Agents Chemother 2008;52(1):299–305.
[13] Schagen F, Moor A, Cheong S, Cramer S, van Ormondt H, van der Eb A. Photodynamic treatment of adenoviral vectors with visible light: an easy and convenient method for viral inactivation. Gene Ther 1999;6(5):873–6.
[14] Cormick MP, Alvarez MG, Rovera M, Durantini EN. Photodynamic inactivation of *Candida albicans* sensitized by tri- and tetra-cationic porphyrin derivatives. Eur J Med Chem 2009;44(4):1592–9.
[15] Kim S, Kwon O, Park J. Inactivation of catalase and superoxide dismutase by singlet oxygen derived from photoactivated dye. Biochimie 2001;83(5):437–44.
[16] Wainwright M, Phoenix D, Laycock S, Wareing D, Wright P. Photobactericidal activity of phenothiazinium dyes against methicillin-resistant strains of *Staphylococcus aureus*. FEMS Microbiol Lett 1998;160(2):177–81.
[17] Parsons C, McCoy CP, Gorman SP, Jones DS, Bell SEJ, Brady C, et al. Anti-infective photodynamic biomaterials for the prevention of intraocular lens-associated infectious endophthalmitis. Biomaterials 2009 2;30(4):597–602.
[18] Henderson BA, Grimes KJ. Blue-blocking IOLs: a complete review of the literature. Surv Ophthalmol 2010;55(3):284–9.
[19] Cruickshanks KJ, Klein R, Klein BE, Nondahl DM. Sunlight and the 5-year incidence of early age-related maculopathy: the Beaver Dam Eye Study. Arch Ophthalmol 2001;119(2):246–50.
[20] Grimm C, Wenzel A, Williams TP, Rol PO, Hafezi F, Remé CE. Rhodopsin-mediated blue-light damage to the rat retina: effect of photoreversal of bleaching. Invest Ophthalmol Vis Sci 2001;42(2):497–505.
[21] Brockmann C, Schulz M, Laube T. Transmittance characteristics of ultraviolet and blue-light filtering intraocular lenses. J Cataract Refract Surg 2008;34(7):1161–6.
[22] Wainwright M. Photodynamic antimicrobial chemotherapy (PACT). J Antimicrob Chemother 1998;42:13–28.
[23] Jones D, McLaughlin D, McCoy C, Gorman S. Physicochemical characterisation and biological evaluation of hydrogel-poly(epsilon-caprolactone) interpenetrating polymer networks as novel urinary biomaterials. Biomaterials 2005;26(14):1761–70.
[24] Jones D, McGovern J, Woolfson A, Adair C, Gorman S. Physicochemical characterization of hexetidine-impregnated endotracheal tube poly(vinyl chloride) and resistance to adherence of respiratory bacterial pathogens. Pharm Res 2002;19(6):818–24.
[25] Jones D, Bonner M, Gorman S, Akay M, Keane P. Sequential polyurethane-poly(methylmethacrylate) interpenetrating polymer networks as ureteral biomaterials: mechanical properties and comparative resistance to urinary encrustation. J Mater Sci Mater Med 1997;8(11):713–7.
[26] Jones D, Djokic J, McCoy C, Gorman S. Poly(epsilon-caprolactone) and poly(epsilon-caprolactone)-polyvinylpyrrolidone-iodine blends as ureteral biomaterials: characterisation of mechanical and surface properties, degradation and resistance to encrustation in vitro. Biomaterials 2002;23(23):4449–58.
[27] Gorman S, Jones D, Bonner M, Akay M, Keane P. Mechanical performance of polyurethane ureteral stents *in vitro* and *ex vivo*. Biomaterials 1997;18(20):1379–83.
[28] Katsikogianni M, Missirlis YF. Concise review of mechanisms of bacterial adhesion to biomaterials and of techniques used in estimating bacteria–material interactions. Eur Cell Mater 2004;8:37–57.
[29] McEldowney S, Fletcher M. Variability of the influence of physicochemical factors affecting bacterial adhesion to polystyrene substrata. Appl Environ Microbiol 1986;52(3):460–5.
[30] Demidova T, Hamblin M. Effect of cell-photo sensitizer binding and cell density on microbial photoinactivation. Antimicrob Agents Chemother 2005;49(6):2329–35.
[31] Gottenbos B, van der Mei H, Klatter F, Grijpma D, Feijen J, Nieuwenhuis P. Positively charged biomaterials exert antimicrobial effects on gram-negative bacilli in rats. Biomaterials 2003;24(16):2707–10.
[32] Gottenbos B, Grijpma D, van der Mei H, Feijen J, Busscher H. Antimicrobial effects of positively charged surfaces on adhering Gram-positive and Gram-negative bacteria. J Antimicrob Chemother 2001;48(1):7–13.
[33] Hamblin M, Hasan T. Photodynamic therapy: a new antimicrobial approach to infectious disease? Photochem Photobiol Sci 2004;3(5):436–50.
[34] Jori G, Brown S. Photosensitized inactivation of microorganisms. Photochem Photobiol Sci 2004;3(5):403–5.
[35] Jackson T, Eykyn S, Graham E, Stanford M. Endogenous bacterial endophthalmitis: a 17-year prospective series and review of 267 reported cases. Surv Ophthalmol 2003;48(4):403–25.